Trivalent nanobody-based ligands mediate powerful activation of GPVI, CLEC-2 and PEAR1 in human platelets whereas FcγRIIA requires a tetravalent ligand

Martin, Eleyna; Clark, Joanne; Montague, Samantha; Moran, Luis A; Di, Ying; Bull, Lily J; Whittle, Luke; Raka, Florije; Buka, Richard; Zafar, Idrees; Kardeby, Caroline; Slater, Alexandre; Watson, Steve

DOI:
10.1016/j.jtha.2023.09.026

Received: 7 August 2023 | Revised: 19 September 2023 | Accepted: 27 September 2023

https://doi.org/10.1016/j.jtha.2023.09.026

ORIGINAL ARTICLE

Trivalent nanobody-based ligands mediate powerful activation of GPVI, CLEC-2, and PEAR1 in human platelets whereas FcγRIIA requires a tetravalent ligand

Eleyna M. Martin[1] | Joanne C. Clark[1,2] | Samantha J. Montague[1] | Luis A. Morán[1] | Ying Di[1] | Lily J. Bull[1] | Luke Whittle[1] | Florije Raka[3] | Richard J. Buka[1] | Idrees Zafar[1] | Caroline Kardeby[1,4] | Alexandre Slater[1] | Steve P. Watson[1,2]

[1]Institute of Cardiovascular Sciences, University of Birmingham, Edgbaston, Birmingham, UK

[2]Centre of Membrane Proteins and Receptors (COMPARE), The Universities of Birmingham and Nottingham, The Midlands, UK

[3]Institute for Transfusion Medicine-Skopje, Skopje, North Macedonia

[4]Current address: School of Biosciences, College of Health and Life Sciences, Aston University, Birmingham, UK

Correspondence
Eleyna M. Martin and Steve P. Watson, Institute of Cardiovascular Sciences, IBR Building, College of Medical and Dental Science, University of Birmingham, Edgbaston, Birmingham, UK, B15 2TT.
Email: e.martin.2@bham.ac.uk and s.p.watson@bham.ac.uk

Funding information
This work was funded by the Wellcome Trust Joint Investigator award (204951/Z/16Z).

Abstract

Background: Clustering of the receptors glycoprotein receptor VI (GPVI), C-type lectin-like receptor 2 (CLEC-2), low-affinity immunoglobulin γ Fc region receptor II-a (FcγRIIA), and platelet endothelial aggregation receptor 1 (PEAR1) leads to powerful activation of platelets through phosphorylation of tyrosine in their cytosolic tails and initiation of downstream signaling cascades. GPVI, CLEC-2, and FcγRIIA signal through YxxL motifs that activate Syk. PEAR1 signals through a YxxM motif that activates phosphoinositide 3-kinase. Current ligands for these receptors have an undefined valency and show significant batch variation and, for some, uncertain specificity.

Objectives: We have raised nanobodies against each of these receptors and multimerized them to identify the minimum number of epitopes to achieve robust activation of human platelets.

Methods: Divalent and trivalent nanobodies were generated using a flexible glycine-serine linker. Tetravalent nanobodies utilize a mouse Fc domain (IgG2a, which does not bind to FcγRIIA) to dimerize the divalent nanobody. Ligand affinity measurements were determined by surface plasmon resonance. Platelet aggregation, adenosine triphosphate secretion, and protein phosphorylation were analyzed using standardized methods.

Results: Multimerization of the nanobodies led to a stepwise increase in affinity with divalent and higher-order nanobody oligomers having sub-nanomolar affinity. The trivalent nanobodies to GPVI, CLEC-2, and PEAR1 stimulated powerful and robust platelet aggregation, secretion, and protein phosphorylation at low nanomolar concentrations. A tetravalent nanobody was required to activate FcγRIIA with the concentration-response relationship showing a greater variability and reduced

Manuscript handled by: Katsue Suzuki-Inoue

Final decision: Katsue Suzuki-Inoue, 28 September 2023

Eleyna M. Martin, Joanne C. Clark, Samantha J. Montague and Luis A. Morán contributed equally to this work.

sensitivity compared with the other nanobody-based ligands, despite a sub-nanomolar binding affinity.

Conclusion: The multivalent nanobodies represent a series of standardized, potent agonists for platelet glycoprotein receptors. They have applications as research tools and in clinical assays.

KEYWORDS
cell signaling, ligands, platelets, Src kinases, tyrosine kinase-linked receptors

1 | INTRODUCTION

The 3 platelet immune receptors: glycoprotein receptor VI (GPVI), C-type lectin-like receptor 2 (CLEC-2), and low-affinity immunoglobulin γ Fc region receptor II-a (FcγRIIA), and the related platelet endothelial aggregation receptor 1 (PEAR1), regulate many of the nonhemostatic functions of platelets including inflammation and host defense. They are implicated in a variety of thrombotic disorders in both the arterial and venous systems making them targets for a new class of anti-platelet therapies. Targeting these receptors is predicted to have a minimal effect on bleeding compared with current cyclooxygenase and $P2Y_{12}$ receptor antagonists [1–4].

The tyrosine kinase-linked receptors GPVI and FcγRIIA signal via an immunoreceptor tyrosine-based activation motif (ITAM) which consists of 2 YxxL motifs. The binding of the tandem SH2 domains in Syk to the conserved phosphorylated tyrosine residues within the ITAM initiates downstream signaling. FcγRIIA has one ITAM in its cytoplasmic tail, while in GPVI, the ITAM is present in each chain of the associated Fc receptor γ-chain (FcRγ) homodimer. In contrast, CLEC-2 signals via a single YxxL known as a hemITAM, with Syk crosslinking YxxLs on 2 receptor chains. The activation of Syk by all 3 receptors leads to the activation of PLCγ2 [3,5–7].

PEAR1 is a receptor for sulfated polysaccharides, including fucoidans and heparin, and the extracellular matrix protein SVEP1 [8–10]. PEAR1 has a single YxxM that is phosphorylated by Src kinases, and which binds the tandem SH2 domains of the regulatory subunit of phosphoinositide 3-kinase (PI3K). This generates a signaling cascade that leads to activation of the serine-threonine kinase Akt [11,12]. Several of the more common variants associated with cardiovascular disease increase PEAR1 expression [1].

All 4 glycoprotein receptors are "activated" by multivalent ligands which drive a critical density of intracellular motifs in the inner leaflet of the membrane for phosphorylation by constitutively active kinases. Currently, we have a rudimentary understanding of the relationship between cluster size and signal generation, and how this relates to platelet activation. This includes not only the number of ligand epitopes required to induce platelet activation but also the contribution of receptor dimerization and crosslinking of cytosolic tails to receptor clustering [12–14].

One contributing factor to this limited understanding is the absence of activating ligands of known valency to all 4 platelet glycoprotein receptors, with the current ligands having uncertain stoichiometries and significant batch variation [15–17]. In addition, some of these bind to other receptors as exemplified by the binding of collagen to integrin α2β1 [18–22]. While synthetic collagen-related peptides based on a repeated glycine-proline-hydroxyproline (GPO) tri-peptide core backbone are specific to GPVI, they are a mixture of dimers, trimers, and higher-order oligomers [23,24]. The widely used ligand for CLEC-2, rhodocytin, is a snake venom toxin predominantly thought to be an $(\alpha\beta)_2$ tetramer but which has been shown to polydisperse in solution and form high-order multimers [25–27]. The endogenous ligand for CLEC-2, podoplanin, is a single transmembrane-spanning protein that is unable to cluster CLEC-2 unless expressed on a surface [28]. The low-affinity Fc receptor, FcγRIIA, is activated by immune complexes or crosslinked antibodies, and PEAR1 by heavily sulfated ligands. In both cases, there is heterogeneity and batch variation in ligand composition [29–31].

Recently, we have shown that human platelets can be activated by crosslinked, tetravalent nanobodies to GPVI and CLEC-2 [13,14]. In contrast, divalent nanobodies to both receptors are unable to induce activation and block the response to tetravalent ligands, suggesting they function as antagonists [13,14]. In the present study, we have generated crosslinked, trivalent nanobodies to GPVI and CLEC-2 and extended this approach to PEAR1 and FcγRIIA, to determine the minimal ligand valency required to cause platelet activation via these receptors. We showed that trivalent nanobodies stimulate potent and robust activation of GPVI, CLEC-2, and PEAR1 in all donors. In contrast,

Essentials

- Current ligands of platelet glycoprotein receptors have undefined valency and batch variation.
- Trivalent nanobodies activate glycoprotein receptor VI, C-type lectin-like receptor 2, and platelet endothelial aggregation receptor 1 at low nanomolar concentrations.
- A tetravalent nanobody activates low-affinity immunoglobulin γ Fc region receptor II-a with wide variation in potency between donors.
- Multivalent nanobodies are standardized ligands for use as research tools and in clinical assays.

a tetravalent nanobody is required to activate FcγRIIA while the trivalent nanobody (based on the same nanobody subunit) is an antagonist to the tetravalent ligand. The novel nanobody-based ligands represent a new class of agent to study mechanisms of receptor activation for the development of validated clinical assays, to study platelet dysfunction, and to aid development of novel antiplatelet drugs.

2 | MATERIALS AND METHODS

2.1 | Ethical approvals

Blood sample collection from consenting, healthy volunteers was granted by the University of Birmingham Internal Ethical Review (ERN_11-0175-AP5) in accordance with the Declaration of Helsinki.

2.2 | Materials

Prostacyclin (#18220) was purchased from *Caymen Chemicals*. Thrombin from bovine plasma (#T4648), indomethacin (#I7378), and ticagrelor (#SML2482) were purchased from *Merck*. Collagen-related peptide was purchased from *CambCol Laboratories*. PRT-060318 (#SYN-1204) was purchased from *Caltag Medsystems*. Dasatinib (#D-3307) was purchased from *LC laboratories*. TGX 221 (#5832) was purchased from *Tocris Bioscience*. AYP1 Fab was made in house from the monoclonal antibody (mAb), AYP1, as previously described [14].

2.3 | Generation of nanobodies

Nanobodies targeted against the extracellular domain of platelet receptors GPVI, CLEC-2, FcγRIIA, and PEAR1 were generated in collaboration with *VIB Nanobody Core*. The recombinant human proteins used as antigens were as follows: GPVI D1D2-Fc (residues 21-183, IgG1 Fc region), CLEC-2 ECD (residues 55-229, N-terminal his_6-tag), PEAR1 EGF-like repeats 12-13 (residues 567-651, C-terminal his_6-tag), and FcγRIIA Ig-domains (residues 37-217, C-terminal his_6-tag). Further details can be found in Supplementary Methods. Screening revealed GPVI/CLEC-2/FcγRIIA/PEAR1 positive colonies of which 54/46/83/24 represented unique nanobody sequences belonging to 33/12/13/2 different CDR3 groups, respectively. The library of clones was provided by VIB as *Escherichia coli* TG1 harboring phagemid pMECS-GG containing nanobody genes.

2.4 | Generation of multivalent nanobodies

Divalent nanobody constructs were created using a short flexible $(GGGGS)_3$ linker between 2 copies of the original nanobody protein sequence, as previously described for GPVI and CLEC-2 and were expressed in bacteria [13,14,32]. The trivalent nanobodies were made using the same crosslinking method and were expressed in mammalian cells, as described below. The tetravalent nanobodies were generated by addition of a mouse Fc domain (IgG2a) at the C-terminus of the respective divalent nanobody. The divalent, trivalent, and tetravalent nanobodies were named as shown in Table 1. Generation of the plasmid DNA was outsourced to VIB Nanobody Core.

TABLE 1 Nomenclature for multivalent nanobodies against GPVI, CLEC-2, PEAR1 and FcγRIIA.

Name	Receptor	Valency
Nb2	GPVI	Monovalent
Nb2-2	GPVI	Divalent
Nb2-3	GPVI	Trivalent
Nb2-2-Fc	GPVI	Tetravalent (m IgG2a Fc)
LUAS	CLEC-2	Monovalent
LUAS-2	CLEC-2	Divalent
LUAS-3	CLEC-2	Trivalent
LUAS-2-Fc	CLEC-2	Tetravalent (m IgG2a Fc)
Nb138	PEAR1	Monovalent
Nb138-2	PEAR1	Divalent
Nb138-3	PEAR1	Trivalent
Nb138-2-Fc	PEAR1	Tetravalent (m IgG2a Fc)
Nb17	FcγRIIA	Monovalent
Nb17-2	FcγRIIA	Divalent
Nb17-3	FcγRIIA	Trivalent
Nb17-2-Fc	FcγRIIA	Tetravalent (m IgG2a Fc)

CLEC-2, C-type lectin-like receptor 2; FcγRIIA, low-affinity immunoglobulin γ Fc region receptor II-a; GPVI, glycoprotein receptor VI; PEAR1, platelet endothelial aggregation receptor 1.

2.5 | Expression and purification of nanobodies from mammalian HEK293T cells

Tri- and tetravalent nanobody DNA received in the pSS1 vector contains an N-terminal BCL1 signal sequence that targets the nanobody for secretion from the cells, allowing their extraction from the cell culture media. Mammalian HEK293T cells were cultured at 37 °C and 5% CO_2 in complete Dulbecco's modified Eagle's medium supplemented with 10% fetal bovine serum, 1% penicillin, 1% streptomycin, and 1% glutamine. Tri- and tetravalent nanobody DNA was transiently transfected at 60% cell confluency using polyethylenimine (PEI Max MW 40 000, Polysciences) according to the manufacturer's instructions. Nanobodies were expressed as secreted protein into the culture media, collected after 7 days, and subsequently purified using affinity chromatography using either nickel NTA beads for the trivalent nanobodies or a MabSelect SuRe column (Cytiva) for the Fc-tetravalent nanobodies. Tag cleavage was achieved as described for the divalent nanobodies [13,14]. Further purification by size exclusion chromatography on a HiLoad 26/600 Superdex 75 pg column (Cytiva)

was used, if necessary, to obtain pure nanobodies. The concentration of purified nanobody was determined using a NanoDrop spectrophotometer (ND-1000, Geneflow) measuring absorbance at 280 nm according to the manufacturer's protocol. Purified nanobodies were stored at −80 °C.

2.6 | Surface plasmon resonance

Surface plasmon resonance (SPR) experiments were performed using a Biacore T200 instrument (GE Healthcare). For all experiments, the recombinant human receptor GPVI, CLEC-2, FcγRIIA, or PEAR1 (see above nanobody generation section for specific residues) was immobilized directly onto a CM5 chip using amine-coupling to the carboxylmethylated dextran-coated surface. Reference surfaces were blocked using 1 M ethanolamine at a pH of 8. Each concentration of nanobody was run as follows; 120 second injection, 300- to 900-second dissociation, 30-second regeneration with 10 mM glycine at a pH of 1.5 followed by a 300-second stabilization period. All sensorgrams shown are double reference subtracted and at least 2 replicates were injected per cycle as well as experimental replicates of n = 3. Experiments were performed at 25 °C with a flow rate of 30 μL/min in HBS-EP running buffer (0.01 M HEPES, pH = 7.4; 0.15 M NaCl, 3 mM EDTA, 0.005% v/v surfactant P20). Multi-cycle kinetic assays were used with at least 5 concentration points between 0.1× and 10× the predicted K_D. Kinetic analysis was performed using the Biacore T200 Evaluation software using a global fitting to a 1:1 binding model and presented as mean ± SEM.

2.7 | Preparation of human platelets

Blood was collected in trisodium citrate (3.8% w/v 1:9 blood) by venipuncture and platelet-rich plasma (PRP) was obtained by centrifugation at 200 × g, 20 minutes. For washed platelets, the anticoagulant acid citrate dextrose (1:9) was added to blood prior to centrifugation then platelets were isolated from the PRP by a second centrifugation at 1000 × g, 10 minutes in the presence of prostacyclin (2.8 μM) followed by resuspension in modified Tyrode's buffer (129 mM NaCl, 0.34 mM Na_2HPO_4, 2.9 mM KCl, 12 mM $NaHCO_3$, 20 mM HEPES, 1 mM $MgCl_2$, 5 mM glucose, pH = 7.3) to the desired concentration. Platelet count was determined using a Beckman Coulter counter. For aggregation measurements, platelets were used at 2×10^8 cells/mL and for protein phosphorylation measurements platelets were used at 4×10^8 cells/mL.

2.8 | Light transmission aggregometry and luminescence measurement of adenosine triphosphate secretion

Aggregation was monitored by light transmission aggregometry using Chrono-Log aggregometers (model 700, 490 4+4 and 460VS; Chrono-Log Corporation, UK) at 37 °C with constant stirring at 1200 rpm. Platelets were pre-treated for 3 minutes with inhibitors prior to addition of agonist. Aggregation was recorded over 10 minutes after the addition of agonist or nanobody. Secretion of adenosine triphosphate (ATP) was measured on a Chrono-Log Lumi-dual model 460VS aggregometer at 37 °C with constant stirring at 1200 rpm using luciferin-luciferase Chrono-lume reagent (7.5% v/v; Chrono-Log Corporation). Secretion was recorded for 10 minutes after addition of agonist, and then calibration of ATP secretion was achieved by addition of ATP standard (2 nM).

2.9 | Platelet lysis and measurement of protein phosphorylation

Whole cell lysates were prepared as previously described [8]. Primary antibodies used and their working concentrations were as follows; anti-phosphotyrosine 4G10 (1:1000), phospho-PLCγ2 Tyr 1217 (1:250), phospho-Syk Tyr 525/526 (1:500), phospho-AKT Ser473 (1:1000), and GAPDH antibody (1:1000). Secondary antibodies were used and their working concentrations were as follows: anti-mouse IgG horse-radish peroxidase (1:10 000) and anti-rabbit IgG horse-radish peroxidase (1:10 000). A more detailed description can be found in the Supplementary Methods.

2.10 | Statistical analysis

Statistical analysis was performed using GraphPad Prism 9 (version 9.4.1). Aggregation data are presented as mean ± SD. Data were tested for normality by Shapiro–Wilk test and statistical significance was calculated using one-way analysis of variance or Kruskal–Wallis as appropriate, with Dunnett's *post hoc* test for multiple comparisons. P values of <.05 were considered statistically significant.

3 | RESULTS

3.1 | Multivalent nanobodies against GPVI, CLEC-2, PEAR1, and FcγRIIA can be produced at high yield and purity

The nanobodies to GPVI, CLEC-2, and PEAR1 were raised and characterized as described previously [8,14,32]. Furthermore, 83 nanobodies from 13 structural classes (based on their CDR3 domains) were raised against the 2 IgG domains in FcγRIIA and screened against the recombinant protein used for their generation. The most potent nanobodies to each receptor were selected for dimerization using a standard 15-amino acid length glycine-serine $(GGGGS)_3$ linker. The following nanobodies were selected: Nb2 (GPVI); Nb4 (renamed LUAS; CLEC-2); Nb138 (PEAR1); and Nb17 (FcγRIIA). This approach was extended to create the trivalent variants. Tetravalent nanobodies were generated by crosslinking of 2 divalent nanobodies using a

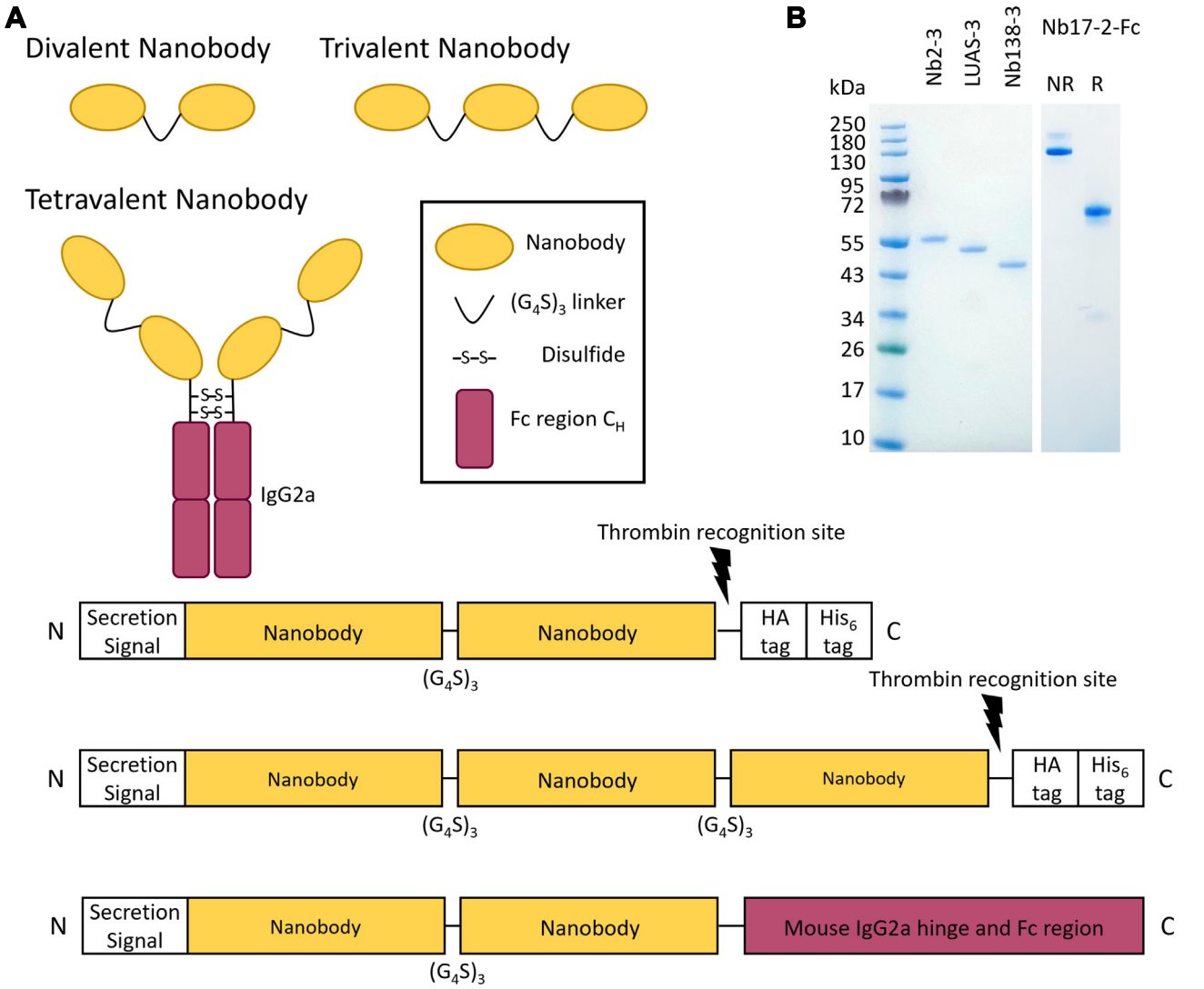

FIGURE 1 Generation of multivalent nanobodies against the platelet receptors GPVI, CLEC-2, PEAR1, and FcγRIIA. (A) The architecture of the di-, tri-, and tetravalent nanobodies is shown. The pelB leader sequence or SSBLC1 signal sequence was added to the N-terminus of the multivalent nanobodies to enable the secretion of the product from bacterial and mammalian cells, respectively. A mouse IgG2a hinge and Fc region were utilized to form the tetravalent nanobody. The di- and trivalent nanobodies contain C-terminal purification tags that are cleaved by thrombin to form the final product. (B) SDS-PAGE showing purity of the multivalent nanobodies. Color pre-stained protein standard is shown on the left. The following molecular weights are predicted: Nb2-3 (43.7 kDa), LUAS-3 (42.8 kDa), Nb138-3 (38.4 kDa), and Nb17-2-Fc (107.8 kDa, 53.9 kDa reduced) shown from left to right. NR, non-reducing conditions; R, reducing conditions. Fc-tetravalent nanobodies appear as a doublet on SDS-PAGE due to the flexible nature of the protein.

mouse IgG2a hinge and Fc region, noting that mouse IgG2a does not bind to human FcγRIIA [33]. The divalent nanobodies were expressed from bacteria at 0.5-2 mg yield per L of growth (*E. coli* WK6). The tri- and tetravalent nanobodies were expressed in mammalian HEK293T cells with 5-10 mg protein per liter of culture media. The schematic representation and domain architecture for the multivalent nanobodies is depicted in Figure 1A. The nomenclature of the multimerized nanobodies is shown in Table 1. Representative SDS-PAGE showing purity of the trivalent (GPVI, CLEC-2, and PEAR1) and tetravalent (FcγRIIA) nanobody variants is shown in Figure 1B. The presence of doublet bands for the Fc-linked tetravalent constructs on SDS-PAGE may reflect either the flexible nature of the glycine-serine linkers or differential glycosylation of the Fc domains, as the proteins elute as single peaks during size exclusion chromatography (not shown). A similar level of purity was achieved with the other nanobody variants (Supplementary Figures S2–S5).

3.2 | SPR reveals sub-nanomolar receptor-nanobody binding affinities

To determine the binding affinities of the newly generated multivalent nanobodies to their respective receptors, we performed SPR experiments. The divalent, trivalent, and tetravalent nanobodies for GPVI,

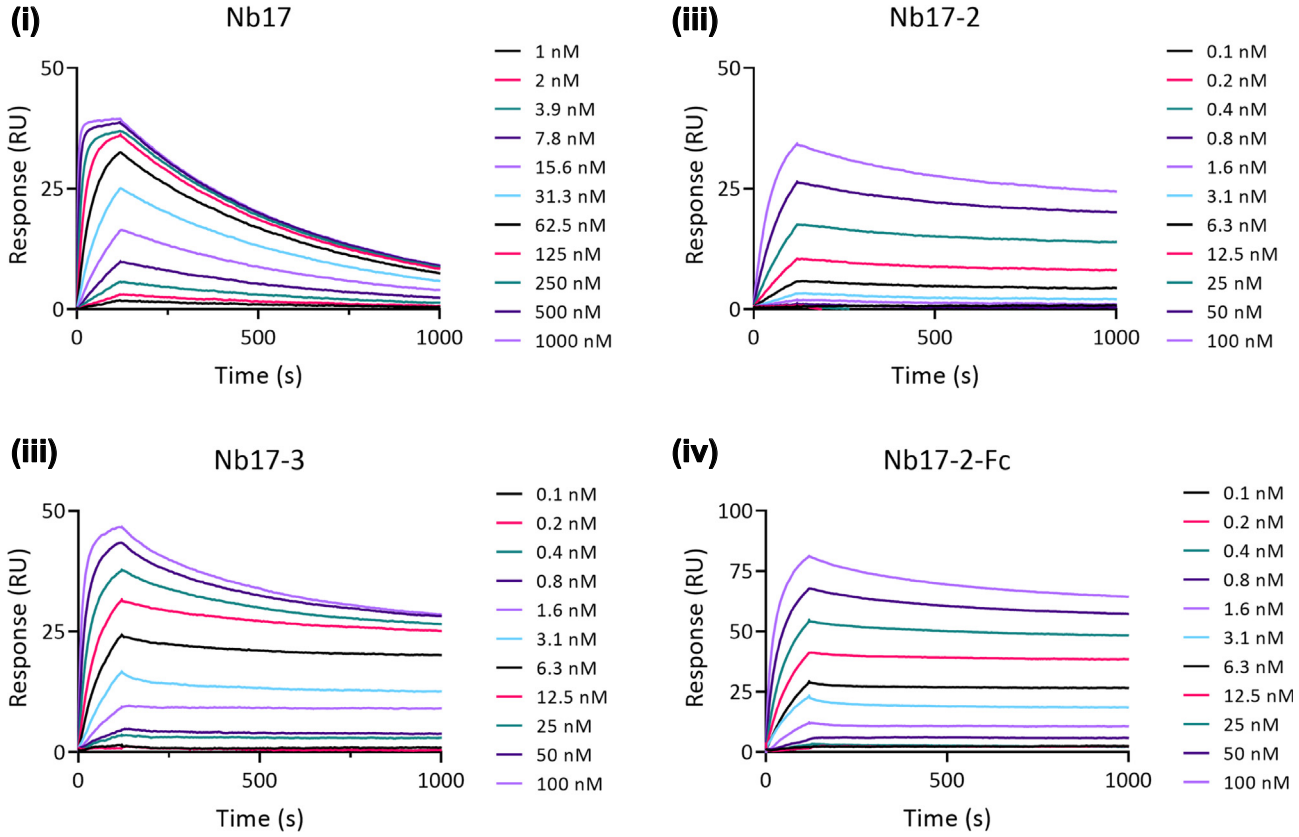

FIGURE 2 Surface plasmon resonance measurements for nanobody variants binding to the FcγRIIA receptor. Surface plasmon resonance (SPR) was used to determine the binding affinity of each nanobody to its respective receptor. Representative sensorgrams showing a concentration series of (i) Nb17, (ii) divalent Nb17-2, (iii) trivalent Nb17-3, and (iv) tetravalent Nb17-2-Fc flowed across a surface of the receptor (recombinant human Ig domains of FcγRIIA); color key is shown on the right for each experiment. All sensorgrams are double reference subtracted. Kinetic parameters were determined using a global fitting model in the BIAEvaluation software, with calculated KD values reported in Table 2. *N* = 3 independent experiments.

CLEC-2, PEAR1, and FcγRIIA gave sub-nanomolar binding affinities. Representative sensorgrams for Nb17 variants are displayed in Figure 2 and calculated K_D values are presented in Table 2 [34]; the sensorgrams for the other nanobody variants are presented in Supplementary Figure S1. The affinities of the monovalent nanobodies ranged from sub-nanomolar to over 100 nanomolar, while multimerization lead to a stepwise increase in affinity due to the added effect of avidity (Table 2). This was particularly marked for the monovalent nanobodies to CLEC-2 and PEAR1 with dimerization increasing the K_D values by 2 orders of magnitude (Supplementary Figure S1 and Table 2). The increase in affinity upon multimerization is evidence that the nanobodies are able to bind to multiple copies of their immobilized receptors.

3.3 | Tri- and tetravalent Nb2 variants stimulate platelet activation via GPVI

We have previously reported that the divalent nanobody-based ligand to GPVI, Nb2-2, is a potent antagonist of collagen-induced aggregation of human platelets [13]. In contrast, the trivalent variant of Nb2, Nb2-3, stimulated rapid and sustained aggregation of washed platelets with an EC_{50} value of 0.98 nM (*n* = 10, 95% CI, 0.51-1.21; Figure 3A). Dose-response curves were similar between donors with the greatest variation in response observed at a submaximal concentration of 1 nM. A similar dose-response relationship was observed for the tetravalent nanobody, Nb2-2-Fc, with a slightly lower EC_{50} of 0.75 nM (*n* = 10, 95% CI, 0.67-0.86) and a more robust response at 1 nM (Supplementary Figure S2). The small increase in potency and reproducibility in response at 1 nM is likely to be due to the additional epitope and a greater level of receptor clustering. The trivalent and tetravalent nanobodies also stimulated aggregation in PRP with similar dose-response relationships to those in washed platelets (Figure 3A; not shown).

We next investigated the ability of the trivalent nanobody to stimulate secretion of ATP. Nb2-3 stimulated rapid and robust secretion of ATP in washed platelets and in PRP with a similar maximal response to that induced by classical agonists such as thrombin and collagen-related peptide (Figure 3B). The dose-response curves were similar and slightly positioned to the right of those for aggregation as seen with classical platelet agonists (Supplementary Figure S2).

TABLE 2 Binding affinity values for nanobody-receptor interactions calculated by surface plasmon resonance.

Nanobody	Receptor	K_D (nM)
Nb2	GPVI	0.58 ± 0.06
Nb2-2	GPVI	0.1 ± 0.003
Nb2-3	GPVI	0.091 ± 0.040
Nb2-2-Fc	GPVI	0.024 ± 0.0029
LUAS	CLEC-2	137 ± 7
LUAS-2	CLEC-2	0.67 ± 0.09
LUAS-3	CLEC-2	0.53 ± 0.30
LUAS-2-Fc	CLEC-2	0.25 ± 0.098
Nb138	PEAR1	14.2 ± 2.4
Nb138-2	PEAR1	0.59 ± 0.036
Nb138-3	PEAR1	0.089 ± 0.063
Nb138-2-Fc	PEAR1	0.19 ± 0.036
Nb17	FcγRIIA	4.6 ± 0.0069
Nb17-2	FcγRIIA	0.33 ± 0.027
Nb17-3	FcγRIIA	0.31 ± 0.011
Nb17-2-Fc	FcγRIIA	0.054 ± 0.012

Tabulated K_D calculations for all nanobody variants against the GPVI, CLEC-2, PEAR1, and FcγRIIA receptors, as determined by surface plasmon resonance. Values are mean of 3 independent surface plasmon resonance experiments with SEM shown for each value. Nb2 was raised against a dimeric form of GPVI (D1-D2-Fc), we have previously published the binding affinity determined for the dimeric construct as 0.7 nM [32] and shown that the conformation of GPVI D1-D2 is independent of GPVI dimerization [34]. CLEC-2, C-type lectin-like receptor 2; FcγRIIA, low-affinity immunoglobulin γ Fc region receptor II-a; GPVI, glycoprotein receptor VI; PEAR1, platelet endothelial aggregation receptor 1.

The Src and Syk inhibitors, dasatinib and PRT-060318, blocked aggregation to a maximally effective concentration of Nb2-3 (10 nM; Figure 3C) consistent with activation of GPVI. Aggregation to Nb2-3 (10 nM) was partially reduced in the presence of the $P2Y_{12}$ and cyclooxygenase inhibitors, ticagrelor and indomethacin, respectively, and almost blocked by their combination demonstrating an important feedback role for the 2 secondary agonists adenosine diphosphate (ADP) and thromboxane A_2 (TxA_2) (Figure 3C). The divalent nanobody to GPVI, Nb2-2, blocked aggregation to Nb2-3 (Figure 3C) as a direct binding interface inhibitor. Nb2-3 stimulated a marked increase in tyrosine phosphorylation in whole cell lysates which included the signaling proteins Syk and PLCγ2 (Figure 3C). The increase in phosphorylation in whole cell lysates was blocked by dasatinib and reduced by PRT-060318 (Figure 3C), as expected and previously shown for GPVI ligands. The increase in tyrosine phosphorylation occurred within 30 seconds and was sustained for 10 minutes (Supplementary Figure S2).

These results demonstrate that trivalent and tetravalent nanobodies stimulate potent platelet activation through GPVI and that this is reproducible across donors.

3.4 | Tri- and tetravalent LUAS variants stimulate platelet activation via CLEC-2

We have previously reported that the divalent nanobody-based ligand to CLEC-2, LUAS-2, is a powerful antagonist against rhodocytin-induced aggregation of human platelets [14]. In contrast, the trivalent nanobody, LUAS-3, stimulated and sustained aggregation of washed platelets with a similar rapid onset of aggregation and pattern of response to that of Nb2-3 against GPVI (Figure 4A). The EC_{50} value for aggregation was 1.79 nM (n = 10, 95% CI, 0.47-2.82; Figure 4A). The dose-response curves were similar between donors with the greatest variation in response at 1 nM (Figure 4). The tetravalent nanobody to CLEC-2, LUAS-2-Fc, also induced rapid and sustained aggregation with a slightly lower EC_{50} of 0.53 nM (n = 10, 95% CI, 0.47-0.72; Supplementary Figure S3) consistent with the higher affinity as measured by SPR (Table 2). LUAS-3 also stimulated aggregation in PRP with a similar dose-response relationship to that in washed platelets (Figure 4A). LUAS-3 stimulated rapid and reproducible secretion of ATP in washed platelets and PRP with the dose-response curves lying slightly positioned right to that for aggregation (Figure 4B).

As with the trivalent nanobody to GPVI, aggregation induced by LUAS-3 was blocked in the presence of dasatinib and PRT-060318, reduced in the presence of ticagrelor and indomethacin, and abrogated in their combined presence (Figure 4C). Aggregation was also blocked by the Fab of the CLEC-2 mAb AYP1 (Figure 4C). LUAS-3 stimulated a marked increase in tyrosine phosphorylation including the signaling proteins Syk and PLCγ2; the increase in phosphorylation in whole cell lysates was blocked in the presence of dasatinib and reduced in the presence of PRT-060318 (Figure 4C). LUAS-3 stimulated an increase in tyrosine phosphorylation at 30 seconds and this was sustained for 10 minutes (Supplementary Figure S3).

These results demonstrate that, as with the tri- and tetravalent nanobodies to GPVI, the tri- and tetravalent nanobody-based ligands to CLEC-2 stimulate potent platelet activation which is reproducible between donors.

3.5 | Di-, tri-, and tetravalent Nb138 variants stimulate platelet activation via PEAR1

We have previously reported that sulfated ligands to PEAR1 induce powerful activation of human platelets which can be blocked by a PEAR1 nanobody, Nb138, raised against the EGF-like repeats 12-13 in the receptor [8]. We have crosslinked Nb138 to generate divalent, trivalent, and tetravalent variants and showed that these have a stepwise increase in affinity for PEAR1 as determined by SPR (Table 2).

The divalent form of Nb138, Nb138-2, stimulated platelet aggregation but with a wide variation in potency between donors (Supplementary Figure S4) with the majority of donors only responding to concentrations of 30 nM and above. In contrast, the trivalent Nb, Nb138-3, stimulated rapid and reproducible platelet

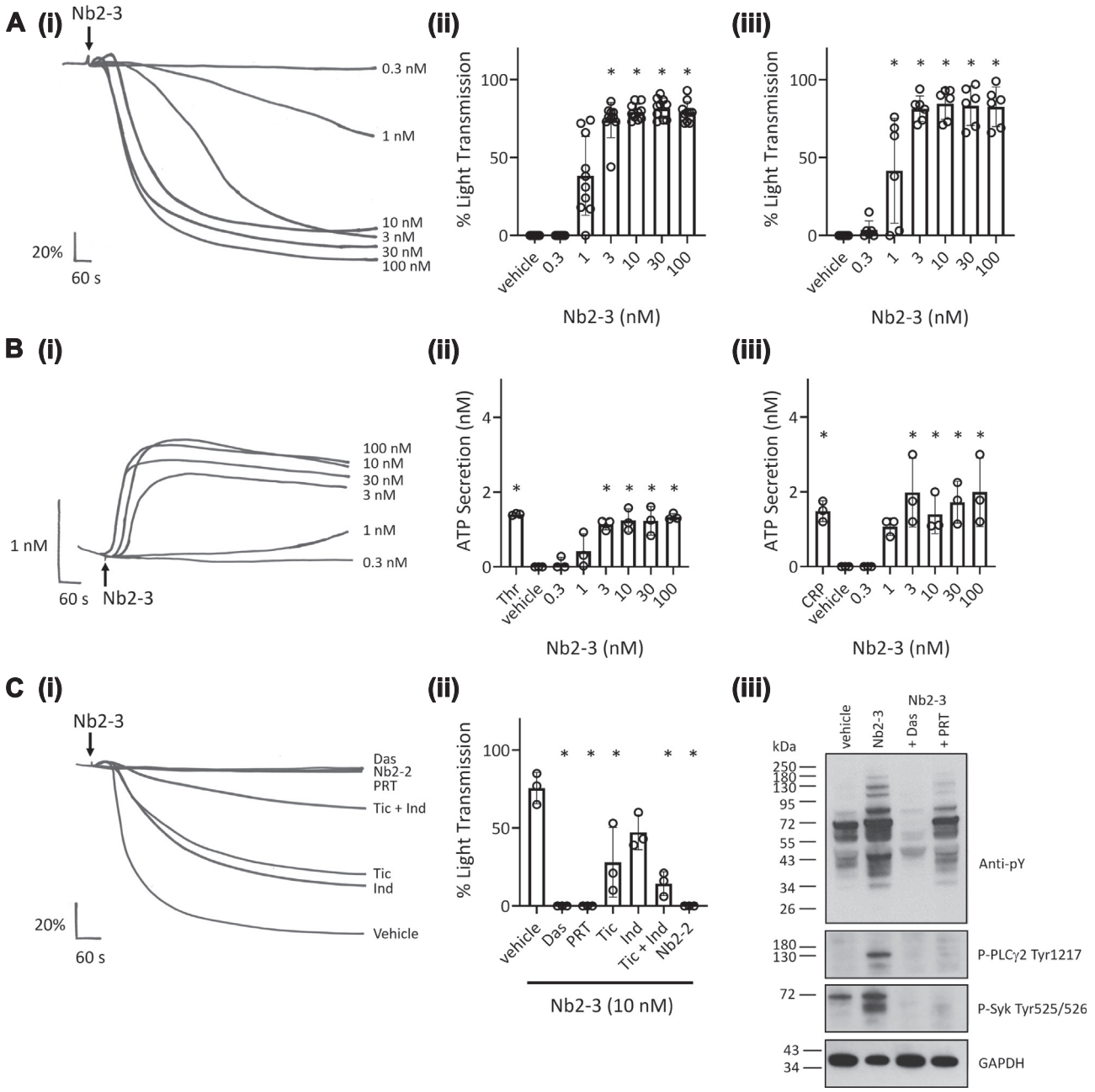

FIGURE 3 A trivalent nanobody, Nb2-3, stimulates the activation of platelets via GPVI. (A)(i) Representative traces of aggregation using washed platelets stimulated by a trivalent nanobody to GPVI, Nb2-3. Arrows indicate the addition of agonist. Quantification of maximal aggregation at 10 minutes post agonist addition for (ii) washed platelets (n = 10) and (iii) platelet-rich plasma; n = 6. (B) Representative traces of ATP secretion, measured using luciferin/luciferase, using washed platelets activated by Nb2-3. Arrows indicate the addition of agonist. Quantification of ATP secretion in comparison to an ATP standard, presented in nM, in (ii) washed platelets, and (iii) Platelet-rich plasma. N = 3. Thr: thrombin (0.1 U/mL); CRP: collagen-related peptide (10 μg/mL) and vehicle: dimethyl sulfoxide (0.01% v/v). (C) The effect of inhibitors on platelet aggregation. (i) Representative traces of Nb2-3-induced platelet aggregation in the presence and absence of: Src inhibitor dasatinib (Das, 10 μM), Syk inhibitor PRT-060318 (PRT, 1 μM), P2Y12 inhibitor ticagrelor (Tic, 1 μM), cyclooxygenase inhibitor indomethacin (Ind, 1 μM), combined P2Y12 and cyclooxygenase inhibitors (Tic + Ind), and GPVI inhibitor Nb2-2 (100 nM). (ii) Quantification of maximal aggregation at 10 minutes post addition of agonist shown in washed platelets. N = 3. (iii) Representative image of western blots showing anti-phosphotyrosine staining of platelet lysates stimulated using Nb2-3 in the presence and absence of inhibitors. dasatinib and PRT-060318. N = 3. Data are shown as mean ± SD analyzed by one-way analysis of variance, or Kruskal–Wallis for A(ii), compared to vehicle control with Dunnett's *post hoc* test for multiple comparisons. * = $P < .05$.

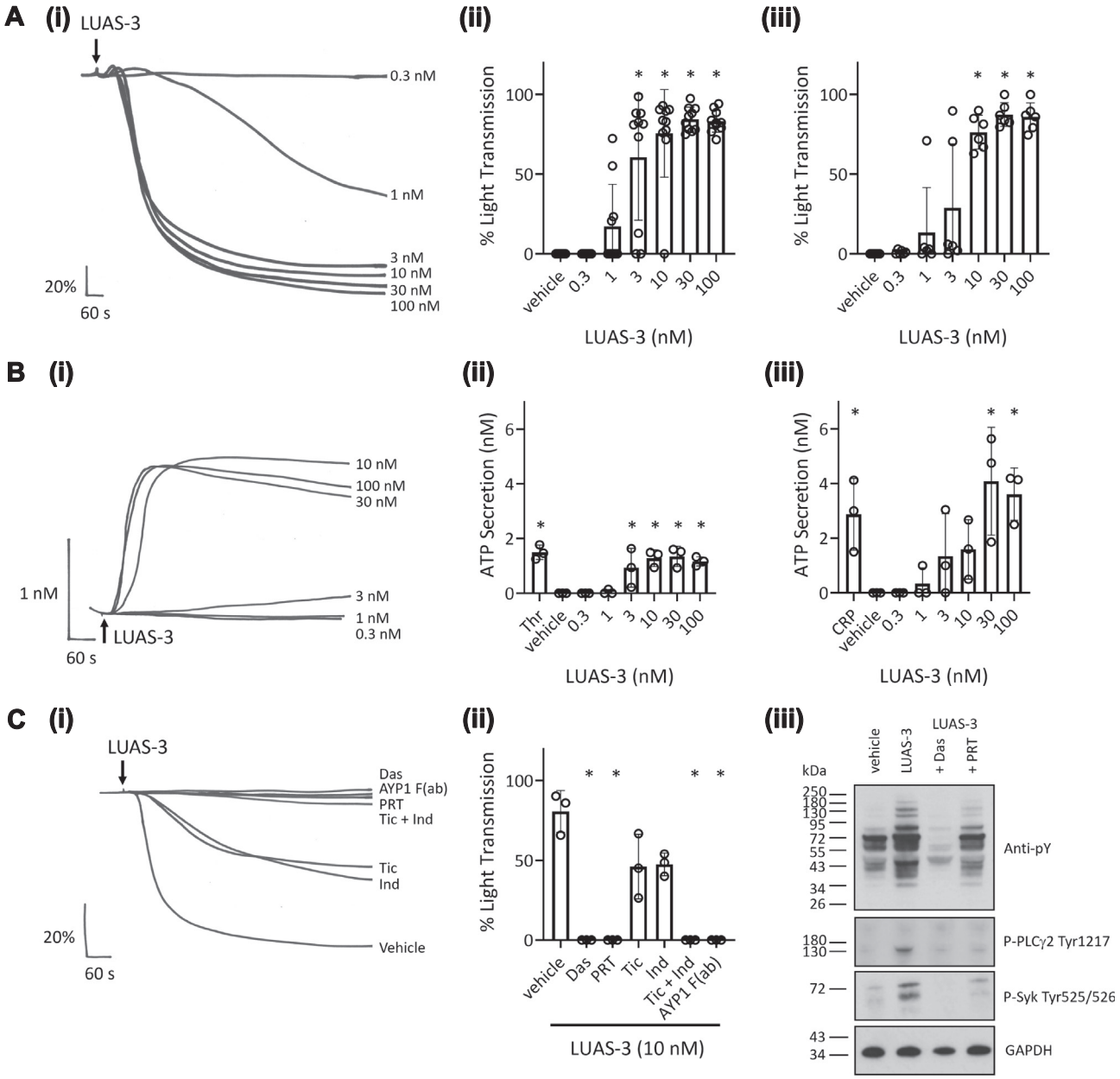

FIGURE 4 Trivalent LUAS-3 induces activation of platelets via CLEC-2. (A)(i) Representative traces of aggregation using washed platelets stimulated by a trivalent nanobody to CLEC-2, LUAS-3. Arrows indicate addition of agonist. Quantification of maximal aggregation at 10 minutes post agonist addition for (ii) washed platelets (n = 10) and (iii) platelet-rich plasma (n = 6). (B) Representative traces of ATP secretion, measured using luciferin/luciferase, using washed platelets activated by LUAS-3. Arrows indicate addition of agonist. Quantification of ATP secretion in comparison to an ATP standard, presented in nM, in (ii) washed platelets and (iii) Platelet-rich plasma. N = 3. Thr: thrombin (0.1 U/mL); CRP: collagen-related peptide (10 μg/mL); and vehicle: dimethyl sulfoxide (0.1% v/v). (C) The effect of inhibitors on platelet activation. (i) Representative traces of LUAS-3-induced platelet aggregation in the presence and absence of Src inhibitor dasatinib (Das, 10 μM), Syk inhibitor PRT-060318 (PRT, 1 μM), P2Y12 inhibitor ticagrelor (Tic, 1 μM), cyclooxygenase inhibitor indomethacin (Ind, 1 μM), combined P2Y12 and cyclooxygenase inhibitors (Tic + Ind), and CLEC-2 inhibitor AYP1 Fab (208 nM). (ii) Quantification of maximal aggregation at 10 minutes post addition of agonist shown in washed platelets. N = 3. (iii) Representative image of western blots showing anti-phosphotyrosine staining of platelet lysates stimulated using LUAS-3 in the presence and absence of inhibitors dasatinib and PRT060318. N = 3. Data are shown as mean ± SD analyzed by one-way analysis of variance, or Kruskal–Wallis for C(ii), compared to vehicle control with Dunnett's *post hoc* test for multiple comparisons. * = $P < .05$.

aggregation in all donors with an EC_{50} value of 0.65 nM (n = 10, 95% CI, 0.23-1.44; Figure 5A). The tetravalent variant, Nb138-2-Fc, also stimulated powerful and reproducible platelet activation (Supplementary Figure S4). Nb138-3 stimulated aggregation in PRP with a similar dose-response curve to washed platelets (Figure 5A). The PEAR1 nanobodies caused little to no secretion (results not shown), in concordance with recently published data on heparin-induced PEAR1 activation [8].

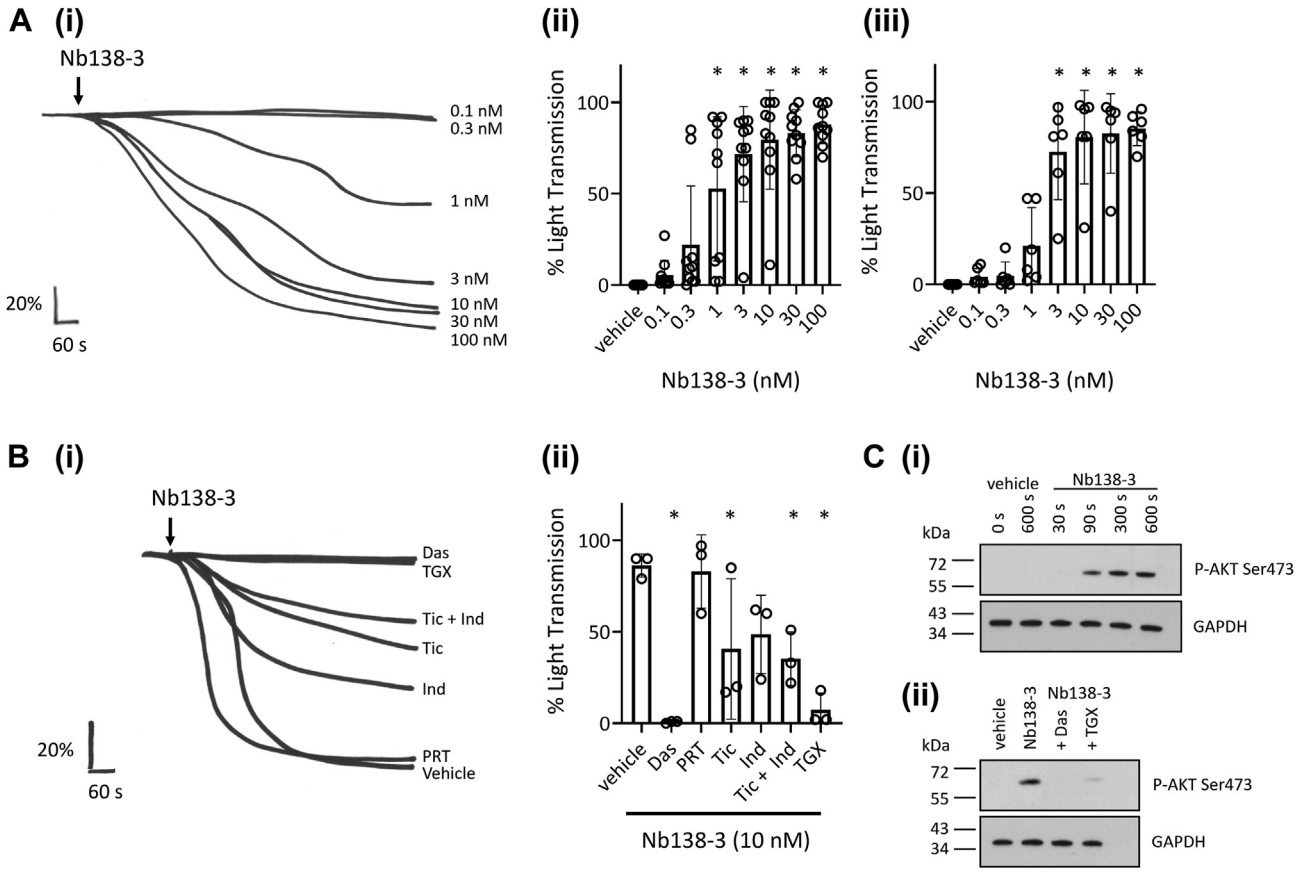

FIGURE 5 Trivalent Nb138-3 is an agonist for PEAR1-mediated platelet activation. (A)(i) Representative traces of aggregation using washed platelets stimulated by a trivalent nanobody to PEAR1, Nb138-3. Arrows indicate addition of agonist. Quantification of maximal aggregation at 10 minutes post agonist addition for (ii) washed platelets (n = 10) and (iii) platelet-rich plasma (n = 6). Thr: thrombin (0.1 U/mL); CRP: collagen-related peptide (10 μg/mL); and vehicle: dimethyl sulfoxide (0.01% v/v). (B) The effect of inhibitors on platelet activation. (i) Representative traces of Nb138-3-induced platelet aggregation in the presence and absence of Src inhibitor dasatinib (Das, 10 μM), Syk inhibitor PRT-060318 (PRT, 1 μM), P2Y12 inhibitor ticagrelor (Tic, 1 μM), cyclooxygenase inhibitor indomethacin (Ind, 1 μM), combined P2Y12 and cyclooxygenase inhibitors (Tic + Ind), and PI3K inhibitor TGX 221 (TGX, 500 nM). (ii) Quantification of maximal aggregation at 10 minutes post addition of agonist shown in washed platelets. N = 3. (C) Representative image of western blots showing anti-phospho AKT staining of platelet lysates stimulated using Nb138-3. (i) Time course of phosphorylation of PI3K in response to Nb138-3 (10 nM) stimulation. N = 3. (ii) Phosphorylation in the presence and absence of inhibitors dasatinib and TGX 221. N = 3. Data are shown as mean ± SD analyzed by one-way analysis of variance compared with vehicle control, with Dunnett's *post hoc* test for multiple comparisons. * = $P < .05$.

In contrast to GPVI and CLEC-2, PEAR1 signals through a Src-PI3K-Akt-dependent pathway, with the Src kinase phosphorylating a conserved YxxM sequence in the cytosolic tail of PEAR1 leading to binding of the regulatory unit of PI3K [35]. Activation is independent of the tyrosine kinase Syk. In line with these results, aggregation induced by Nb138-3 was blocked by the Src and PI3K inhibitors, dasatinib and TGX 221, respectively, but was unaltered in the presence of the Syk inhibitor, PRT-060318 (Figure 5B). Aggregation was also reduced in the presence of ticagrelor and indomethacin, or in their combined presence, demonstrating the contribution of the 2 feedback agonists (Figure 5B). As expected, Nb138-3 stimulated phosphorylation of Akt, measured using a phospho-Akt Ser473-specific antibody. An increase in phosphorylation was observed at 90 seconds and was sustained for 10 minutes (Figure 5C). Phosphorylation of Akt was blocked by dasatinib and TGX 221 (Figure 5C).

These results confirm that Nb138-3 mediates potent platelet activation directly through PEAR1. While a divalent ligand is able to induce activation, a consistent response in all donors was only observed in response to the trivalent ligand.

3.6 | Tetravalent Nb17-2-Fc induces platelet activation via FcγRIIA

Nb17 was selected as one of the most potent nanobodies raised against the recombinant IgG domains of FcγRIIA (Table 2) and crosslinked using the flexible $(GGGGS)_3$ linker to generate divalent and trivalent variants. The divalent variant, Nb17-2, was unable to induce platelet aggregation, and the trivalent ligand, Nb17-3, induced aggregation in one of the 10 donor platelets at a high-nanomolar concentration (Supplementary Figure S5). In contrast, the

tetravalent ligand, Nb17-2-Fc, stimulated aggregation in all donors with an EC_{50} value of 11.7 nM (n = 10, 95% CI, 8.6-17.2; Figure 6A), although in 5 donors, a concentration of 30 nM, and in one donor a concentration of 100 nM was required to induce aggregation. Nb17-2-Fc stimulated the aggregation in PRP with a similar dose-response relationship to that in washed platelets for each donor (Figure 6A). Nb17-2-Fc also stimulated the secretion of ATP in washed platelets and in PRP, again with similar dose-response curves for each donor (Figure 6B).

As with the trivalent nanobody ligands to GPVI and CLEC-2, the stimulation of aggregation by Nb17-2-Fc was completely inhibited by the Src and Syk inhibitors, dasatinib, and PRT-060318 (Figure 6C). Aggregation was reduced in the presence of ticagrelor and indomethacin and blocked by their combination, showing that aggregation is reinforced by the 2 feedback agonists (Figure 6C). Aggregation was also blocked by the trivalent ligand, Nb17-3 (Figure 6C), confirming that activation was mediated through direct FcγRIIA binding. In line with this, Nb17-2-Fc (30 nM) stimulated a marked increase in tyrosine phosphorylation in whole cell lysates including the signaling proteins Syk and PLCγ2 (Figure 6C). The increase in phosphorylation in whole cell lysates was blocked in the presence of dasatinib and reduced in the presence of PRT-060318 (Figure 6C). The increase in phosphorylation was observed at 30 seconds and sustained up to 10 minutes (Supplementary Figure S5).

These results demonstrate that in contrast to the crosslinked nanobodies for GPVI, CLEC-2, and PEAR1, a minimum of 4 binding epitopes is required to stimulate platelet activation through FcγRIIA.

4 | DISCUSSION

This study reports the development and characterization of multivalent nanobody-based ligands for the platelet glycoprotein receptors GPVI, CLEC-2, FcγRIIA, and PEAR1. The di-, tri-, and tetravalent nanobodies have sub-nanomolar affinities for all 4 receptors as shown by SPR, with the affinity increasing in accordance with the valency. While the affinities of the parent monovalent nanobodies varied by 2 orders of magnitude, with those to CLEC-2 and PEAR1 in the high-nanomolar range, the multivalent nanobodies had similar, sub-nanomolar affinities emphasizing the contribution of avidity to the overall affinity.

As expected, the monovalent nanobodies to all 4 receptors had no effect on platelet activation as they are unable to cluster their corresponding receptors and function as competitive antagonists to ligands that bind at the same site, including activating multivalent nanobodies [8,13,14,36]. The divalent nanobodies to GPVI, CLEC-2, and FcγRIIA are similarly unable to induce activation and function as competitive antagonists [8,13,14,32]. The, $F(ab')_2$ fragments of the mAbs to CLEC-2 (AYP1) and FcγRIIA (IV.3), and the whole mAb to GPVI (JAQ1) are also antagonists in human platelets [14,37,38]. These results demonstrate that the dimerization of the 3 ITAM receptors is unable to generate a signal of sufficient strength to drive aggregation, and that divalent ligands are more potent relative to their monovalent counterparts due to their greater affinity.

The divalent ligands to the 3 ITAM receptors are also distinct to the monovalent ligands as they are able to induce receptor dimerization and in some cases larger clusters, if the receptors are already dimers. For this reason, we have proposed that the divalent ligands should be described as partial agonists [14]. Indeed, we have shown that a divalent nanobody to CLEC-2, LUAS-2, and a $F(ab')_2$ fragment of the mAb AYP1 are able to stimulate aggregation in mouse platelets, which express a 10-fold higher level of CLEC-2 relative to human platelets, and activate a NFAT reporter assays in high- but not low-expressing DT40 cells, whereas, the multivalent snake toxin is an agonist in all cases [14,39]. This illustrates that the level of receptor expression as a key variable that influences the response to divalent and multivalent ligands. This is a powerful argument against using divalent nanobodies as candidate therapeutic as the levels of receptors vary between donors.

In contrast to the results with divalent ligands to the 3 ITAM receptors, the divalent nanobody to PEAR1, Nb138-2, stimulated aggregation at mid- to high-nanomolar concentrations showing a wide variation in dose-response relationships between donors. PEAR1 signals through a Src-PI3K-Akt pathway unlike the other 3 receptors which signal through Syk. This alone however is unlikely to account for the difference between the receptors as other factors also influence the strength of the intracellular signal, including the level of receptor expression as discussed above. The copy numbers of the 4 receptors in human platelets are within 3-fold: GPVI 3730 + 453 [40], CLEC-2 2000-3700 [36,41], FcγRIIA 1000-1500 [41,42], and PEAR1 1800 [41] but of these, PEAR1 is the only receptor that is also expressed on intracellular membranes suggesting that the level on the cell surface may be significantly lower than the other receptors [1]. Other factors that influence the strength of the intracellular signal include the degree of receptor dimerization in the resting cell and the action of the feedback agonists, ADP and TxA_2. We have recently provided the first quantitative measurements on the level of dimerization of GPVI and CLEC-2 in transfected cell lines using fluorescence correlation spectroscopy and single molecule photobleaching studies of tagged receptors [14,42]. Both proteins are predominantly monomeric with the degree of dimerization increasing on expression, in line with the law of mass action [14,43]. However, we cannot use these techniques on platelets due to their anucleate nature. FcγRIIA has also been proposed to form a non-covalent dimer on the cell surface that resembles V(L)V(H) dimers in a crystal [44,45], but the degree of dimerization in platelets is not known. There is no information on the dimerization of PEAR1 in platelets. It is also difficult to make a comparison of the role of the 2 secondary agonists, ADP and TxA_2, as this is dependent on the concentration of the ligand.

The trivalent nanobodies to GPVI, CLEC-2, and PEAR1 stimulated rapid and sustained platelet activation at low nanomolar concentrations in all donors, with similar dose-response curves in both washed platelets and in PRP showing that they are freely available in plasma. These results show that a valency of 3 is sufficient to induce activation

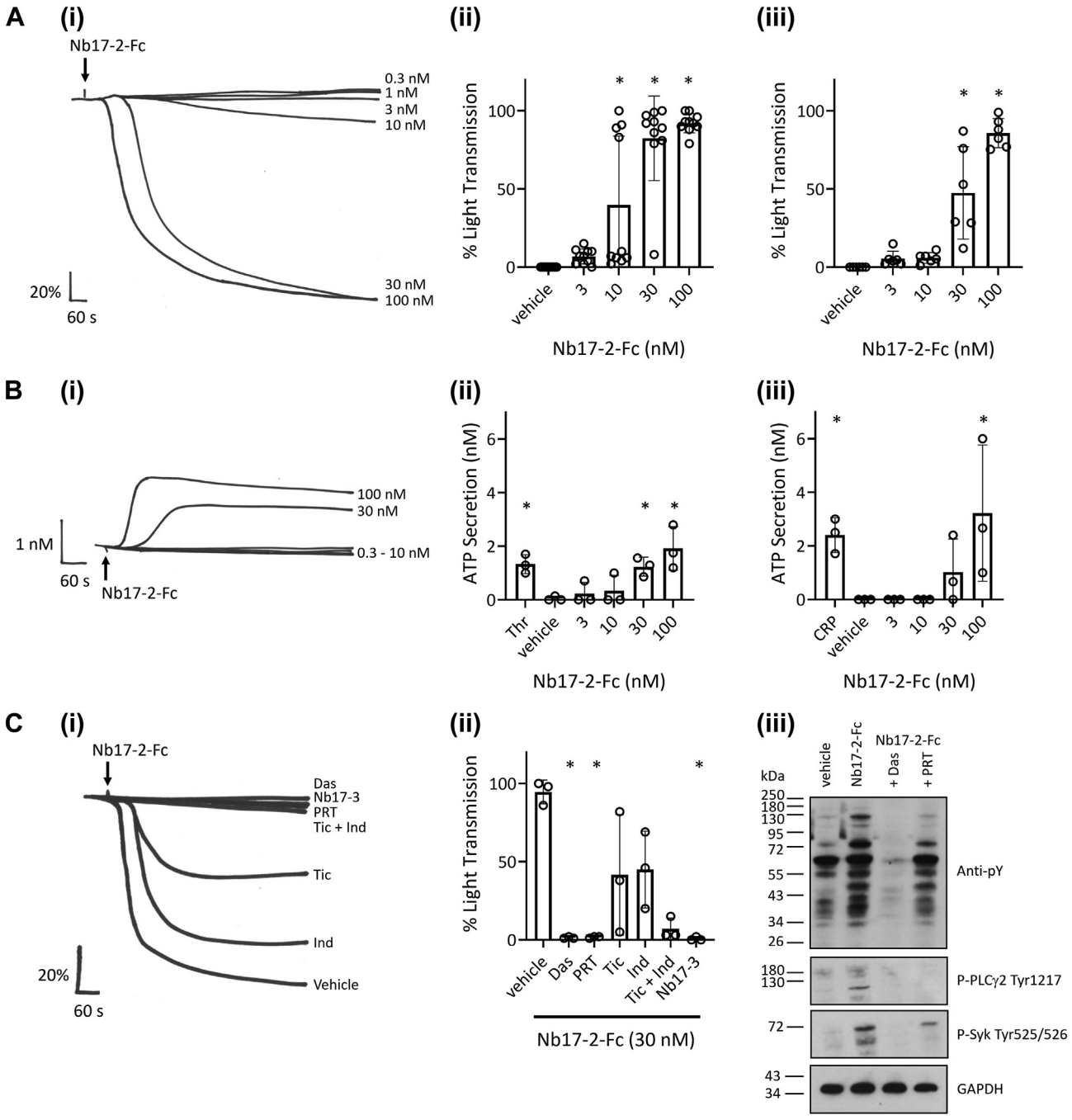

FIGURE 6 A tetravalent nanobody, Nb17-2-Fc, stimulates the activation of platelets via FcγRIIA. (A)(i) Representative traces of aggregation using washed platelets stimulated by a tetravalent nanobody to FcγRIIA, Nb17-2-Fc. Arrows indicate addition of agonist. Quantification of maximal aggregation at 10 minutes post agonist addition for (ii) washed platelets (n = 10) and (iii) platelet-rich plasma (n = 6). (B) Representative traces of ATP secretion, measured using luciferin/luciferase, using washed platelets activated by Nb17-2-Fc. Arrows indicate the addition of agonist. Quantification of ATP secretion in comparison to an ATP standard, presented in nM, in (ii) washed platelets and (iii) Platelet-rich plasma. N = 3. Thr: thrombin (0.1 U/mL); CRP: collagen-related peptide (10 μg/mL); and vehicle: dimethyl sulfoxide (0.1% v/v). (C) The effect of inhibitors on platelet activation. (i) Representative traces of Nb17-2-Fc-induced platelet aggregation in the presence and absence of: Src inhibitor dasatinib (Das, 10 μM), Syk inhibitor PRT-060318 (PRT, 1 μM), P2Y12 inhibitor ticagrelor (Tic, 1 μM), cyclooxygenase inhibitor indomethacin (Ind, 1 μM), combined P2Y12 and cyclooxygenase inhibitors (Tic + Ind), and FcγRIIA blocking agent Nb17-3 (300 nM). (ii) Quantification of maximal aggregation at 10 minutes after the addition of agonist shown in washed platelets. N = 3. (iii) Representative image of western blots showing anti-phosphotyrosine staining of platelet lysates stimulated using Nb17-2-Fc in the presence and absence of inhibitors dasatinib and PRT-060318. N = 3. Data are shown as mean ± SD analyzed by one-way analysis of variance compared with vehicle control, with Dunnett's *post hoc* test for multiple comparisons. * = $P < .05$.

of all 3 receptors. As such, the trivalent ligands represent the first ligands of known stoichiometry for GPVI, CLEC-2, and PEAR1 that produce robust activation of human platelets for application in clinical assays and to further probe the mechanisms underlying receptor activation. Previously, Sasaski et al. [26] (2018) proposed that clustering of at least 4 CLEC-2 receptors was required to elicit activation of human platelets based on results with recombinant forms of the snake venom rhodocytin. A direct comparison to the nanobody-based ligands however is hampered by structural restraints that may prevent engagement of all 4 epitopes in the recombinant snake venom toxin engaging more than 3 receptors. All 3 epitopes in the trivalent nanobody, LUAS-3, can bind to recombinant CLEC-2 as shown by the increase in affinity measured by SPR.

In contrast, in the case of FcγRIIA, a tetravalent nanobody ligand was required to stimulate activation but with a lower EC_{50} value relative to the trivalent ligands and a wider variation in the dose-response curves between donors, despite having a similar affinity as measured by SPR. These observations demonstrate that a higher valency is required for the activation of platelets by FcγRIIA, although whether this is due to the need to induce a greater level of clustering of the low-affinity immune receptor is not known. A marked variation in the sensitivity of activation of platelets by FcγRIIA is also seen in response to serum from patients with heparin-induced thrombocytopenia or vaccine immune-induced thrombocytopenia and thrombosis [46–48]. In both cases, the sera induce activation through the formation of immune complexes formed against platelet factor 4.

The requirement for a minimal ligand valency of 4 to activate FcγRIIA is consistent with the observation that mAbs to the low-affinity immune receptor, which can be considered as trivalent ligands, are unable to activate platelets [38]. On the other hand, mAbs to a wide range of platelet proteins have been shown to induce activation of washed platelets through FcγRIIA, indicating that the low-affinity immune receptor can be activated by heterologous trimeric ligands. This includes mAbs to CLEC-2 [14] and GPVI [49] which are predicted to drive a critical density of YxxL sequences in the membrane for activation of Syk. What is more puzzling however is why mAbs to other receptors that do not have recognized similar motifs, such as the tetraspanin CD9, or are weak of activators of platelets, for example GPIb, are also able to stimulate aggregation [40–52]. One potential explanation is that these proteins may exist in the membrane as higher-order multimers leading to the clustering of FcγRIIA. The ability of the mAbs to induce activation of human platelets is also influenced by the IgG subtype and single nucleotide variants in FcγRIIA [33].

To summarize, we have developed a series of ligands based on crosslinking of nanobodies that can be used to activate the platelet glycoprotein receptors GPVI, CLEC-2, PEAR1, and FcγRIIA. These ligands have advantages over other agonists for these receptors including known valency, high specificity and potency. Therefore, these multivalent nanobodies can be used as research tools to further explore mechanisms of receptor activation and in assays for comparison between laboratories or for development of clinically validated diagnostics to probe platelet function.

AUTHOR CONTRIBUTIONS

E.M.M. designed the research, generated and characterized critical reagents, performed experiments, and analyzed data. J.C.C., S.J.M., L.A.M., Y.D., and C.K. designed the research, performed experiments, and analyzed data. L.J.B., L.W., F.R., R.J.B., and I.Z. performed experiments and analyzed data. A.S. provided intellectual input on reagent expression and characterization. S.P.W. designed the research, reviewed data, and obtained funding. E.M.M., J.C.C., S.J.M., and S.P.W. co-wrote the manuscript. All authors reviewed and approved the manuscript.

ACKNOWLEDGMENTS

This work was funded by the Wellcome Trust Joint Investigator award (204951/Z/16Z). S.P.W. is a BHF Chair (CH03/003). J.C.C., S.J.M., R.J.B., C.K., and A.S. were supported by the Accelerator Award from the BHF (AA/18/2/34218). S.J.M. is supported by a BHF project grant (PG/23/11230). L.A.M. was supported by the European Union's Horizon 2020 research and innovation program under the Marie Sklodowska-Curie grant agreement (766118). C.K. was supported by the European Union's Horizon 2020 research and innovation program under the Marie Sklodowska-Curie grant agreement (893262). We would like to thank Dr Steve Schoonooghe at VIB Nanobody core for assistance in the design and generation of the multivalent nanobody plasmid DNA. This is independent research funded by the providers named above and carried out at the National Institute for Health and Care Research (NIHR) Birmingham Biomedical Research Centre (BRC). The views expressed are those of the authors and not necessarily those of the funders, the NIHR or the Department of Health and Social Care.

DECLARATION OF COMPETING INTERESTS

S.P.W. and A.S. have a patent for the anti-GPVI nanobody Nb2 (WO2022/136457). All other authors declare no conflicts of interest.

REFERENCES

[1] Kardeby C, Damaskinaki FN, Sun Y, Watson SP. Is the endogenous ligand for PEAR1 a proteoglycan: clues from the sea. *Platelets*. 2021;32:779–85.
[2] Harbi MH, Smith CW, Nicolson PLR, Watson SP, Thomas MR. Novel antiplatelet strategies targeting GPVI, CLEC-2 and tyrosine kinases. *Platelets*. 2021;32:29–41.
[3] Rayes J, Watson SP, Nieswandt B. Functional significance of the platelet immune receptors GPVI and CLEC-2. *J Clin Invest*. 2019;129:12–23.
[4] Patel P, Michael JV, Naik UP, McKenzie SE. Platelet FcgammaRIIA in immunity and thrombosis: adaptive immunothrombosis. *J Thromb Haemost*. 2021;19:1149–60.
[5] Qiao J, Al-Tamimi M, Baker RI, Andrews RK, Gardiner EE. The platelet Fc receptor, FcgammaRIIa. *Immunol Rev*. 2015;268:241–52.
[6] Humphrey MB, Lanier LL, Nakamura MC. Role of ITAM-containing adapter proteins and their receptors in the immune system and bone. *Immunol Rev*. 2005;208:50–65.
[7] Martin EM, Zuidscherwoude M, Moran LA, Di Y, Garcia A, Watson SP. The structure of CLEC-2: mechanisms of dimerization and higher-order clustering. *Platelets*. 2021;32:733–43.
[8] Kardeby C, Evans A, Campos J, Al-Wahaibi AM, Smith CW, Slater A, Martin EM, Severin S, Brill A, Pejler G, Sun Y, Watson SP. Heparin

and heparin proteoglycan-mimetics activate platelets via PEAR1 and PI3Kbeta. *J Thromb Haemost*. 2023;21:101–16.
[9] Elenbaas JS, Pudupakkam U, Ashworth KJ, Kang CJ, Patel V, Santana K, Jung IH, Lee PC, Burks KH, Amrute JM, Mecham RP, Halabi CM, Alisio A, Di Paola J, Stitziel NO. SVEP1 is an endogenous ligand for the orphan receptor PEAR1. *Nat Commun*. 2023;14:850.
[10] Nanda N, Bao M, Lin H, Clauser K, Komuves L, Quertermous T, Conley PB, Phillips DR, Hart MJ. Platelet endothelial aggregation receptor 1 (PEAR1), a novel epidermal growth factor repeat-containing transmembrane receptor, participates in platelet contact-induced activation. *J Biol Chem*. 2005;280:24680–9.
[11] Wu H, Windmiller DA, Wang L, Backer JM. YXXM motifs in the PDGF-beta receptor serve dual roles as phosphoinositide 3-kinase binding motifs and tyrosine-based endocytic sorting signals. *J Biol Chem*. 2003;278:40425–8.
[12] Kauskot A, Di Michele M, Loyen S, Freson K, Verhamme P, Hoylaerts MF. A novel mechanism of sustained platelet alphaIIbbeta3 activation via PEAR1. *Blood*. 2012;119:4056–65.
[13] Maqsood Z, Clark JC, Martin EM, Cheung YFH, Morán LA, Watson SET, Pike JA, Di Y, Poulter NS, Slater A, Lange BMH, Nieswandt B, Eble JA, Tomlinson MG, Owen DM, Stegner D, Bridge LJ, Wierling C, Watson SP. Experimental validation of computerised models of clustering of platelet glycoprotein receptors that signal via tandem SH2 domain proteins. *PLoS Comput Biol*. 2022;18:e1010708.
[14] Clark JC, Martin EM, Morán LA, Di Y, Wang X, Zuidscherwoude M, Brown HC, Kavanagh DM, Hummert J, Eble JA, Nieswandt B, Stegner D, Pollitt AY, Herten DP, Tomlinson MG, García A, Watson SP. Divalent nanobodies to platelet CLEC-2 can serve as agonists or antagonists. *Commun Biol*. 2023;6:376.
[15] Jarvis GE, Atkinson BT, Snell DC, Watson SP. Distinct roles of GPVI and integrin alpha(2)beta(1) in platelet shape change and aggregation induced by different collagens. *Br J Pharmacol*. 2002;137:107–17.
[16] Jooss NJ, Henskens YMC, Watson SP, Farndale RW, Gawaz MP, Jandrot-Perrus M, Poulter NS, Heemskerk JWM. Pharmacological inhibition of glycoprotein VI- and integrin alpha2beta1-induced thrombus formation modulated by the collagen type. *Thromb Haemost*. 2023;123:597–612.
[17] Cejas MA, Kinney WA, Chen C, Leo GC, Tounge BA, Vinter JG, Joshi PP, Maryanoff BE. Collagen-related peptides: self-assembly of short, single strands into a functional biomaterial of micrometer scale. *J Am Chem Soc*. 2007;129:2202–3.
[18] Clemetson KJ, Clemetson JM. Platelet collagen receptors. *Thromb Haemost*. 2001;86:189–97.
[19] Emsley J, Knight CG, Farndale RW, Barnes MJ, Liddington RC. Structural basis of collagen recognition by integrin alpha2beta1. *Cell*. 2000;101:47–56.
[20] Cauwenberghs N, Vanhoorelbeke K, Vauterin S, Deckmyn H. Structural determinants within platelet glycoprotein Ibalpha involved in its binding to von Willebrand factor. *Platelets*. 2000;11:373–8.
[21] Tandon NN, Kralisz U, Jamieson GA. Identification of glycoprotein IV (CD36) as a primary receptor for platelet-collagen adhesion. *J Biol Chem*. 1989;264:7576–83.
[22] Moog S, Mangin P, Lenain N, Strassel C, Ravanat C, Schuhler S, Freund M, Santer M, Kahn M, Nieswandt B, Gachet C, Cazenave JP, Lanza F. Platelet glycoprotein V binds to collagen and participates in platelet adhesion and aggregation. *Blood*. 2001;98:1038–46.
[23] Knight CG, Morton LF, Onley DJ, Peachey AR, Ichinohe T, Okuma M, Farndale RW, Barnes MJ. Collagen-platelet interaction: Gly-Pro-Hyp is uniquely specific for platelet Gp VI and mediates platelet activation by collagen. *Cardiovasc Res*. 1999;41:450–7.
[24] Morton LF, Hargreaves PG, Farndale RW, Young RD, Barnes MJ. Integrin alpha 2 beta 1-independent activation of platelets by simple collagen-like peptides: collagen tertiary (triple-helical) and quaternary (polymeric) structures are sufficient alone for alpha 2 beta 1-independent platelet reactivity. *Biochem J*. 1995;306:337–44.
[25] Watson AA, Eble JA, O'Callaghan CA. Crystal structure of rhodocytin, a ligand for the platelet-activating receptor CLEC-2. *Protein Sci*. 2008;17:1611–6.
[26] Sasaki T, Shirai T, Tsukiji N, Otake S, Tamura S, Ichikawa J, Osada M, Satoh K, Ozaki Y, Suzuki-Inoue K. Functional characterization of recombinant snake venom rhodocytin: rhodocytin mutant blocks CLEC-2/podoplanin-dependent platelet aggregation and lung metastasis. *J Thromb Haemost*. 2018;16:960–72.
[27] Hooley E, Papagrigoriou E, Navdaev A, Pandey AV, Clemetson JM, Clemetson KJ, Emsley J. The crystal structure of the platelet activator aggretin reveals a novel (alphabeta)2 dimeric structure. *Biochemistry*. 2008;47:7831–7.
[28] Suzuki-Inoue K. CLEC-2/podoplanin and thromboinflammation. *Blood*. 2017;129:1896–8.
[29] Arman M, Krauel K. Human platelet IgG Fc receptor FcgammaRIIA in immunity and thrombosis. *J Thromb Haemost*. 2015;13:893–908.
[30] Zhang Z, Till S, Jiang C, Knappe S, Reutterer S, Scheiflinger F, Szabo CM, Dockal M. Structure-activity relationship of the pro- and anticoagulant effects of Fucus vesiculosus fucoidan. *Thromb Haemost*. 2014;111:429–37.
[31] Tengdelius M, Kardeby C, Fälker K, Griffith M, Påhlsson P, Konradsson P, Grenegård M. Fucoidan-mimetic glycopolymers as tools for studying molecular and cellular responses in human blood platelets. *Macromol Biosci*. 2017;17.
[32] Slater A, Di Y, Clark JC, Jooss NJ, Martin EM, Alenazy F, Thomas MR, Ariëns RAS, Herr AB, Poulter NS, Emsley J, Watson SP. Structural characterization of a novel GPVI-nanobody complex reveals a biologically active domain-swapped GPVI dimer. *Blood*. 2021;137:3443–53.
[33] Temming AR, Bentlage AEH, de Taeye SW, Bosman GP, Lissenberg-Thunnissen SN, Derksen NIL, Brasser G, Mok JY, van Esch WJE, Howie HL, Zimring JC, Vidarsson G. Cross-reactivity of mouse IgG subclasses to human Fc gamma receptors: antibody deglycosylation only eliminates IgG2b binding. *Mol Immunol*. 2020;127:79–86.
[34] Damaskinaki FN, Jooss NJ, Martin EM, Clark JC, Thomas MR, Poulter NS, Emsley J, Kellam B, Watson SP, Slater A. Characterizing the binding of glycoprotein VI with nanobody 35 reveals a novel monomeric structure of glycoprotein VI where the conformation of D1+D2 is independent of dimerization. *J Thromb Haemost*. 2023;21:317–28.
[35] Kardeby C, Fälker K, Haining EJ, Criel M, Lindkvist M, Barroso R, Påhlsson P, Ljungberg LU, Tengdelius M, Rainger GE, Watson S, Eble JA, Hoylaerts MF, Emsley J, Konradsson P, Watson SP, Sun Y, Grenegård M. Synthetic glycopolymers and natural fucoidans cause human platelet aggregation via PEAR1 and GPIbalpha. *Blood Adv*. 2019;3:275–87.
[36] Gitz E, Pollitt AY, Gitz-Francois JJ, Alshehri O, Mori J, Montague S, Nash GB, Douglas MR, Gardiner EE, Andrews RK, Buckley CD, Harrison P, Watson SP. CLEC-2 expression is maintained on activated platelets and on platelet microparticles. *Blood*. 2014;124:2262–70.
[37] Navarro S, Starke A, Heemskerk JWM, Kuijpers MJE, Stegner D, Nieswandt B. Targeting of a conserved epitope in mouse and human GPVI differently affects receptor function. *Int J Mol Sci*. 2022;23.
[38] Meyer T, Robles-Carrillo L, Davila M, Brodie M, Desai H, Rivera-Amaya M, Francis JL, Amirkhosravi A. CD32a antibodies induce thrombocytopenia and type II hypersensitivity reactions in FCGR2A mice. *Blood*. 2015;126:2230–8.
[39] Brown HC, Beck S, Navarro S, Di Y, Soriano Jerez EM, Kaczmarzyk J, Thomas SG, Mirakaj V, Watson SP, Nieswandt B, Stegner D. Antibody-mediated depletion of human CLEC-2 in a novel humanized mouse model. *Blood Adv*. 2023;7:997–1000.

[40] Best D, Senis YA, Jarvis GE, Eagleton HJ, Roberts DJ, Saito T, Jung SM, Moroi M, Harrison P, Green FR, Watson SP. GPVI levels in platelets: relationship to platelet function at high shear. *Blood*. 2003;102:2811–8.
[41] Burkhart JM, Vaudel M, Gambaryan S, Radau S, Walter U, Martens L, Geiger J, Sickmann A, Zahedi RP. The first comprehensive and quantitative analysis of human platelet protein composition allows the comparative analysis of structural and functional pathways. *Blood*. 2012;120:e73–82.
[42] Kelton JG. The pathophysiology of heparin-induced thrombocytopenia: biological basis for treatment. *Chest*. 2005;127:9S–20S.
[43] Clark JC, Neagoe RAI, Zuidscherwoude M, Kavanagh DM, Slater A, Martin EM, Soave M, Stegner D, Nieswandt B, Poulter NS, Hummert J, Herten DP, Tomlinson MG, Hill SJ, Watson SP. Evidence that GPVI is expressed as a mixture of monomers and dimers, and that the D2 domain is not essential for GPVI activation. *Thromb Haemost*. 2021;121:1435–47.
[44] Powell MS, Barnes NC, Bradford TM, Musgrave IF, Wines BD, Cambier JC, Hogarth PM. Alteration of the Fc gamma RIIa dimer interface affects receptor signaling but not ligand binding. *J Immunol*. 2006;176:7489–94.
[45] Maxwell KF, Powell MS, Hulett MD, Barton PA, McKenzie IF, Garrett TP, Hogarth PM. Crystal structure of the human leukocyte Fc receptor, Fc gammaRIIa. *Nat Struct Biol*. 1999;6:437–42.
[46] Warkentin TE. HIT paradigms and paradoxes. *J Thromb Haemost*. 2011;9:105–17.
[47] Handtke S, Wolff M, Zaninetti C, Wesche J, Schönborn L, Aurich K, Ulm L, Hübner NO, Becker K, Thiele T, Greinacher A. A flow cytometric assay to detect platelet-activating antibodies in VITT after ChAdOx1 nCov-19 vaccination. *Blood*. 2021;137:3656–9.
[48] Montague SJ, Smith CW, Lodwick CS, Stoneley C, Roberts M, Lowe GC, Lester WA, Watson SP, Nicolson PLR. Anti-platelet factor 4 immunoglobulin G levels in vaccine-induced immune thrombocytopenia and thrombosis: persistent positivity through 7 months. *Res Pract Thromb Haemost*. 2022;6:e12707.
[49] Lecut C, Feeney LA, Kingsbury G, Hopkins J, Lanza F, Gachet C, Villeval JL, Jandrot-Perrus M. Human platelet glycoprotein VI function is antagonized by monoclonal antibody-derived Fab fragments. *J Thromb Haemost*. 2003;1:2653–62.
[50] Ozaki Y, Satoh K, Kuroda K, Qi R, Yatomi Y, Yanagi S, Sada K, Yamamura H, Yanabu M, Nomura S, Kume S. Anti-CD9 monoclonal antibody activates p72syk in human platelets. *J Biol Chem*. 1995;270:15119–24.
[51] Cauwenberghs N, Schlammadinger A, Vauterin S, Cooper S, Descheemaeker G, Tornai I, Deckmyn H. Fc-receptor dependent platelet aggregation induced by monoclonal antibodies against platelet glycoprotein Ib or von Willebrand factor. *Thromb Haemost*. 2001;85:679–85.
[52] Nagata H, Nomura S, Sone N, Suzuki M, Kokawa T, Yasunaga K. A new monoclonal CD9 antibody, MALL13, induces platelet activation and cytolysis. *Acta Haematologica Japonica*. 1990;53:1156–71.

SUPPLEMENTARY MATERIAL

The online version contains supplementary material available at https://doi.org/10.1016/j.jtha.2023.09.026